JOC Article

Solvent-Induced Amphiphilic Molecular Baskets: Unimolecular Reversed Micelles with Different Size, Shape, and Flexibility

Eui-Hyun Ryu, Jie Yan, Zhenqi Zhong, and Yan Zhao*

Department of Chemistry, Iowa State University, Ames, Iowa 50011-3111

zhaoy@iastate.edu

Received April 11, 2006

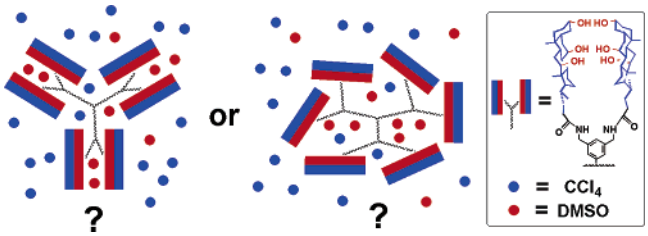

Amphiphilic molecular baskets were obtained by attaching facially amphiphilic cholate groups to a covalent scaffold (calix[4]arene or 1,3,5-2,4,6-hexasubstituted benzene). In a solvent mixture consisting of mostly a nonpolar solvent (i.e., CCl_4) and a polar solvent (i.e., DMSO), the hydrophilic faces of cholates turned inward to form a reversed-micelle-like conformer whose stability was strongly influenced by the number of the cholates and the topology of the scaffold. Preferential solvation of the hydrophilic faces of cholates within the molecule by the polar solvent was cooperative and gave the fundamental driving force to the conformational change. The reversed-micelle-like conformer was most stable in structures that allowed multiple cholates to form a microenvironment that could efficiently enrich the polar solvent molecules from the bulk solvent mixture.

Introduction

Conformations represent different 3-D arrangements of atoms in a molecule as a result of rotations around single bonds. As a molecule adopts different conformations, its size, shape, and distribution of functional groups change simultaneously. Since these properties are intimately related to the physical and chemical behavior of the molecule, conformational control could serve as a rational way to design environmentally responsive materials. This strategy is utilized elegantly by biomolecules such as proteins, whose binding and catalytic functions are frequently regulated through controlled conformational changes.[1] In recent years, foldamers have attracted a great deal of attention of chemists in different fields.[2] As mimics of biomolecules with specific, compact conformations, foldamers may not only shed new light on the folding and functions of biomolecules but also enable chemists to prepare biomolecule-like, stimuli-responsive materials from a bottom-up approach.

Conformational changes in biomolecules may be induced by specific molecules such as an enzyme substrate or an allosteric effector[1] or by general changes in environmental conditions including temperature, pH, and solvent polarity. Response to solvent polarity is not a surprise, as hydrophobic interactions[3] represent a major driving force for the folding of polypeptide chains. An interesting class of biomolecules that display polarity-

* To whom correspondence should be addressed. Phone: (515) 294-5845. Fax: (515) 294-0105.

(1) (a) Koshland, D. E., Jr. *Proc. Natl. Acad. Sci. U.S.A.* **1958**, *44*, 98−104. (b) Koshland, D. E., Jr. *Nat. Med.* **1998**, *4*, 1112−1114. (c) Perutz, M. F. *Mechanisms of Cooperativity and Allosteric Regulation in Proteins*; Cambridge University Press: Cambridge, 1990. (e) Hervé, G., Ed. *Allosteric Enzymes*; CRC Press: Boca Raton, FL, 1989. (e) Kvamme, E.; Pihl, A., Eds. *Regulation of Enzyme Activity and Allosteric Interactions*; Academic Press: New York, 1968.

(2) For several recent reviews, see: (a) Gellman, S. H. *Acc. Chem. Res.* **1998**, *31*, 173−180. (b) Kirshenbaum, K.; Zuckermann, R. N.; Dill, K. A. *Curr. Opin. Struct. Biol.* **1999**, *9*, 530−535. (c) Hill, D. J.; Mio, M. J.; Prince, R. B.; Hughes, T. S.; Moore, J. S. *Chem. Rev.* **2001**, *101*, 3893−4012. (d) Cubberley, M. S.; Iverson, B. L. *Curr. Opin. Chem. Biol.* **2001**, *5*, 650−653. (e) Sanford, A. R.; Gong, B. *Curr. Org. Chem.* **2003**, *7*, 1649−1659. (f) Martinek, T. A.; Fulop, F. *Eur. J. Biochem.* **2003**, *270*, 3657−3666. (g) Cheng, R. P. *Curr. Opin. Struct. Biol.* **2004**, *14*, 512−520. (h) Huc, I. *Eur. J. Org. Chem.* **2004**, 17−29. (i) Licini, G.; Prins, L. J.; Scrimin, P. *Eur. J. Org. Chem.* **2005**, 969−977.

(3) (a) Tanford, C. *The Hydrophobic Effect: Formation of Micelles and Biological Membranes*, 2nd ed.; Wiley: New York, 1980. (b) Ben-Mailm, A. *Hydrophobic Interactions*; Plenum Press: New York, 1980. (c) Dill, K. A. *Biochemistry* **1990**, *29*, 7133−7155. (e) Blokzijl, W.; Engberts, J. B. F. N. *Angew. Chem., Int. Ed. Engl.* **1993**, *32*, 1545−1579.

10.1021/jo0607663 CCC: $33.50
Published on Web 08/19/2006

induced conformational changes is α-helical antimicrobial peptides.[4] These small peptides typically assume random conformations in water but change to amphipathic α-helical structures (which are surface active and can destabilize the membrane) in contact with bacterial membranes, a much less polar environment. In fact, polarity-induced conformational change is important to many biological processes including the translocation of proteins across membranes.[5]

We have been interested in using cholic acid[6] as a building block to construct both foldamers[7] and nonfoldamers[8,9] whose conformations and properties can be reversibly switched. With its large steroid backbone and oppositely facing hydrophilic and hydrophobic groups,[10] cholic acid is uniquely suited for solvophobically driven conformational changes. Previously, we synthesized an amphiphilic molecular basket by coupling cholates to a cone-shaped, aminocalix[4]arene scaffold.[8] The molecule adopted micelle-like conformations in polar solvents with the hydrophilic (α) faces turned outward and reversed-micelle-like conformations in nonpolar solvents with the α faces inward. In this paper, we extend the concept to prepare a series of cholate baskets with different size, shape, and flexibility. We were able to experimentally verify preferential solvation, which had been speculated to drive the conformational changes in the molecular basket. We also found an interesting correlation between the stability of the reversed-micelle-like conformer and the ability for the cholates to form a microenvironment to concentrate polar solvents from a mostly nonpolar solvent mixture such as 10% DMSO in CCl_4.

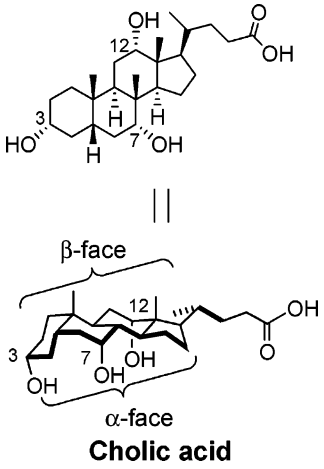

Cholic acid

Results and Discussion

Design and Synthesis of Amphiphilic Molecular Baskets. The geometry of an amphiphile dictates the possible aggregates it can form. For a head/tail amphiphile, spherical micelles (or reversed micelles) are the most common aggregates obtained in water (or nonpolar solvents). With a contrafacial topology, cholate amphiphiles tend to associate through the solvophobic faces into oligomers that resemble micelles and reversed micelles in polar and nonpolar environments, respectively.[11] If several cholates are linked covalently, intramolecular aggregation should happen readily. The difference between inter- and intramolecular aggregation is that cholates can freely approach one another to minimize solvophobic exposure in the former but are restricted by the covalent linkers and the topological scaffold employed in the latter. Therefore, other than concentration independency, unimolecular micelles and reversed micelles[12] from intramolecular aggregation of cholates have the additional advantage of being tuned systematically through structural modification.

The previously reported compound **1a** could encapsulate hydrophobic guests in polar solvents and hydrophilic guests in nonpolar solvents.[9] We were interested in creating larger baskets by insertion of a spacer between the cholates and the calixarene. This is represented by compound **2** with a rigid *p*-aminobenzoyl spacer and **3** with a flexible 4-aminobutyroyl spacer. Ring inversion in calix[4]arene happens readily when the alkyl substituents at the lower rim are smaller than propyl.[13] Compound **1b**, therefore, has a less pre-organized scaffold and is used to test whether solvophobic interactions among the cholates are strong enough to fix the calixarene into one particular conformation. Compounds **5**−**7** are control molecules used in our studies. Most of these compounds were synthesized in a straightforward fashion by amide coupling between the acids and the corresponding amines. Compounds **2** and **3** were

(4) (a) Hwang, P. M.; Vogel, H. J. *Biochem. Cell Biol.* **1998**, *76*, 235−246. (c) Hancock, R. E. W.; Chapple, D. S. *Atimicrob. Agents Chemother.* **1999**, *43*, 1317−1323. (d) Epand, R. M.; Vogel, H. J. *Biochim. Biophys. Acta* **1999**, *1462*, 11−28. (e) Tossi, A.; Sandri, L.; Giangaspero, A. *Biopolymers* **2000**, *55*, 4−30. (f) van't Hof, W.; Veerman, E. C.; Helmerhorst, E. J.; Amerongen, A. V. *Biol. Chem.* **2001**, *382*, 597−619.

(5) Cserhåti, T.; Szögyi, M. *Int. J. Biochem.* **1994**, *26*, 1−18, and references therein.

(6) For some examples of supramolecular systems constructed from cholic acid, see: (a) Davis, A. P.; Bonar-Law, R. P.; Sanders, J. K. M. In *Comprehensive Supramolecular Chemistry*; Atwood, J. L., Davis, J. E. D., MacNicol, D. D., Vögtle, F., Eds.; Pergamon: New York, 1996; Vol. 4, Ch. 7, and references therein. (b) Li, Y.; Dias, J. R. *Chem. Rev.* **1997**, *97*, 283−304, and references therein. (c) Maitra, U. *Curr. Sci.* **1996**, *71*, 617−624. (d) Smith, B. D.; Lambert, T. N. *Chem. Commun.* **2003**, 2261−2268, and references therein. (e) Davis, A. P.; Joos, J.-B. *Coord. Chem. Rev.* **2003**, *240*, 143−156, and references therein. (f) Burrows, C. J.; Sauter, R. A. *J. Inclusion Phenom.* **1987**, *5*, 117−121. (g) Janout, V.; Lanier, M.; Regen, S. L. *J. Am. Chem. Soc.* **1996**, *118*, 1573−1574. (h) Ariga, K.; Terasaka, Y.; Sakai, D.; Tsuji, H.; Kikuchi, J.-I. *J. Am. Chem. Soc.* **2000**, *122*, 7835−7836. (i) Werner, F.; Schneider, H.-J. *J. Inclusion Phenom. Macrocyclic Chem.* **2001**, *41*, 37−40. (j) Yoshino, N.; Satake, A.; Kobuke, Y. *Angew. Chem., Int. Ed.* **2001**, *40*, 457−459.

(7) (a) Zhao, Y.; Zhong, Z. *J. Am. Chem. Soc.* **2005**, *127*, 17894−17901. (b) Zhao, Y.; Zhong, Z. *J. Am. Chem. Soc.* **2006**, *128*, 9988−9989.

(8) Ryu, E.-H.; Zhao, Y. *Org. Lett.* **2004**, *6*, 3187−3189.

(9) Zhao, Y.; Ryu, E.-H. *J. Org. Chem.* **2005**, *70*, 7585−7591.

(10) For other examples of facial amphiphiles, see: (a) Stein, T. M.; Gellman, S. H. *J. Am. Chem. Soc.* **1992**, *114*, 3943−3950. (b) Cheng, Y.; Ho, D. M.; Gottlieb, C. R.; Kahne, D.; Bruck, M. A. *J. Am. Chem. Soc.* **1992**, *114*, 7319−7320. (c) Venkatesan, P.; Cheng, Y.; Kahne, D. *J. Am. Chem. Soc.* **1994**, *116*, 6955−6956. (d) McQuade, D. T.; Barrett, D. G.; Desper, J. M.; Hayashi, R. K.; Gellman, S. H. *J. Am. Chem. Soc.* **1995**, *117*, 4862−4869. (e) Broderick, S.; Davis, A. P.; Williams, R. P. *Tetrahedron Lett.* **1998**, *39*, 6083−6086. (f) Isaacs, L.; Witt, D.; Fettinger, J. C. *Chem. Commun.* **1999**, 2549−2550. (g) Taotafa, U.; McMullin, D. B.; Lee, S. C.; Hansen, L. D.; Savage, P. B. *Org. Lett.* **2000**, *2*, 4117−4120. (h) Arnt, L.; Tew, G. N. *J. Am. Chem. Soc.* **2002**, *124*, 7664−7665. (i) Willemen, H. M.; Marcelis, A. T. M.; Sudhölter, E. J. R. *Langmuir* **2003**, *19*, 2588−2591. (j) Elemans, J. A. A. W.; Slangen, R. R. J.; Rowan, A. E.; Nolte, R. J. M. *J. Org. Chem.* **2003**, *68*, 9040−9049. (k) Zhong, Z.; Yan, J.; Zhao, Y. *Langmuir* **2005**, *21*, 6235−6239. (l) Menger, F. M.; Sorrells, J. L. *J. Am. Chem. Soc.* **2006**, *128*, 4960−4961.

(11) *Sterols and Bile Acids*; Danielsson, H., Sjövall J., Eds.; Elsevier: Amsterdam, 1985.

(12) For some recent examples of interconvertable unimolecular micelles and reversed micelles, see: (a) Basu, S.; Vutukuri, D. R.; Shyamroy, S.; Sandanaraj, B. S.; Thayumanavan, S. *J. Am. Chem. Soc.* **2004**, *126*, 9890−9891. (b) Vutukuri, D. R.; Basu, S.; Thayumanavan, S. *J. Am. Chem. Soc.* **2004**, *126*, 15636−15637. (c) Ghosh, S.; Maitra, U. *Org. Lett.* **2006**, *8*, 399−402.

(13) (a) Gutsche, C. D. In *Calixarenes Revisited, Monograph in Supramolecular Chemistry*; Stoddart, J. F., Ed.; Royal Society of Chemistry: Cambridge, 1998; Ch. 4. (b) Mandolini, L.; Ungaro, R., Eds. *Calixarenes in Action*; Imperial College Press: London, 2000; Ch. 1.

SCHEME 1. Synthesis of Compound 8

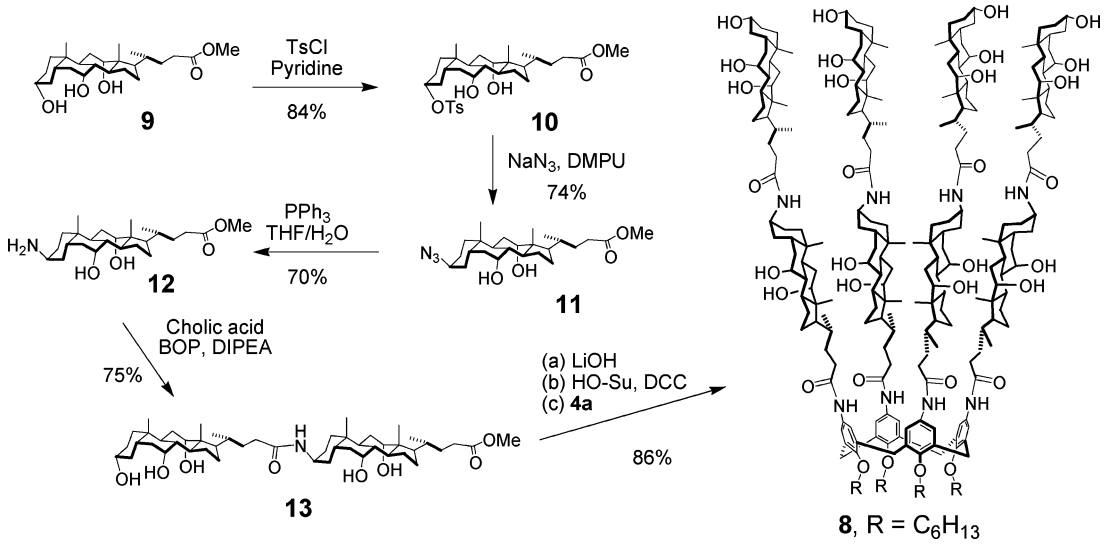

prepared by coupling cholic acid to the spacer first and then the resulting extended acid to calixarene amine **4a**.

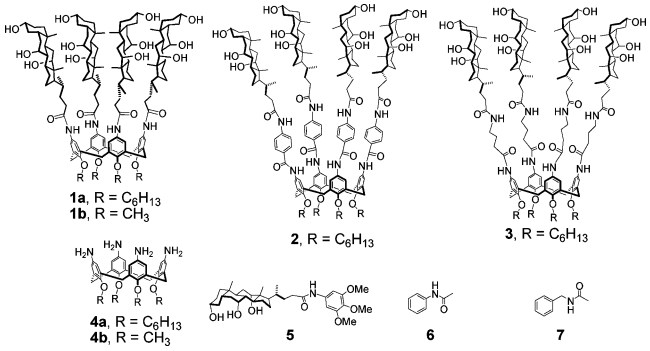

Compound **8** uses cholate dimers as the wall material and thus should contain a deeper capacity. The β-amino cholates are chosen as linkers between the top cholates and the aminocalixarene because the α,β dimer seems to be able to align linearly according to CPK molecular models. (Cholate oligomers consisting of all α linkages are known to fold into helical structures due to the curved backbone.)[7] The synthesis of **8** is outlined in Scheme 1. The terminal hydroxyl group in methyl cholate **9** is more reactive than the other two and was selectively tosylated in pyridine in 85% yield. The tosylate was replaced by azide through a S_N2 reaction and reduced by triphenylphosphine in aqueous THF in 74 and 70% yield, respectively. The amine ester **12** was coupled to cholic acid in the presence of benzotriazol-1-yloxytris(dimethylamino)phosphonium hexafluorophosphate (BOP) and diisopropylethylamine (DIPEA) in 75% yield. The dimer ester **13** was hydrolyzed, converted to the activated *N*-hydroxysuccinimide (HO−Su) ester, and reacted with aminocalixarene **4a** to afford the final product (**8**) in 86% overall yield.

Another scaffold commonly used in supramolecular chemistry is 1,3,5-2,4,6-substituted benzene such as **14**.[14] Because of steric crowdedness, the substituents on the phenyl prefer to alternate up and down around the ring. Using this scaffold, we synthesized a compact tripodal basket **16** as well as several extended baskets with rigid (**17**), flexible (**18**), and β amino cholate (**19**) spacers. A dendritic molecule (**20**) with six arms of cholates was also prepared to increase the width of the basket. It was prepared by coupling the acid derivative of the bis-armed **15** to the triamine scaffold **14**. It should be mentioned that a compound similar to **15** was reported by Burrows and co-workers to form a closed conformation in nonpolar solvents with the two cholates hydrogen bonded to each other.[6f] In our paper, **15** mainly serves as a control to study enrichment of polar solvents within the basket.

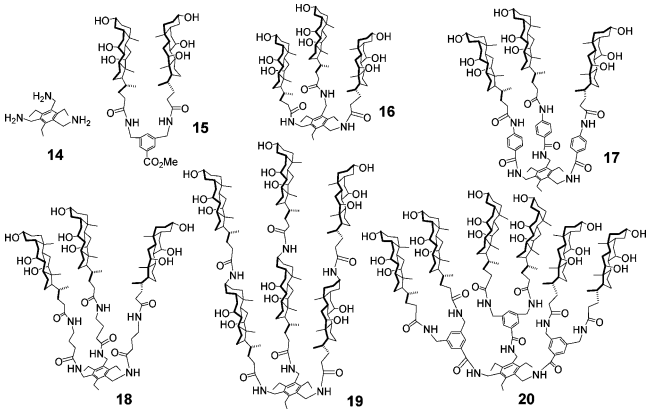

Conformational Changes in Calixarene-Based Molecular Baskets. There were two main lines of evidence for the micelle- and reversed-micelle-like conformations of **1a**. It could bind hydrophobic guests such as pyrene in polar solvent mixtures (e.g., methanol/water = 80:20) and hydrophilic guests such as phenyl β-D-gluocopyranoside in nonpolar mixtures (e.g., methanol/CCl_4 = 5:95).[9] Pyrene caused upfield shifts of the methyl protons on the β faces of cholates, consistent with the micelle-like conformation with inwardly facing β faces. The other line of evidence for the proposed conformations was from ^{1}H NMR data in the absence of guests. The aromatic protons ortho to the amido group appear as a single peak in solvents with intermediate polarity but as two peaks in either polar or nonpolar solvents.[8] The magnitude of splitting was found to correlate with not only solvent polarity but also with the difference of the solvophobicities of the α and β faces of cholates.[8] Such a

(14) Hennrich, G.; Anslyn, E. V. *Chem.—Eur. J.* **2002**, *8*, 2218−2224, and references therein.

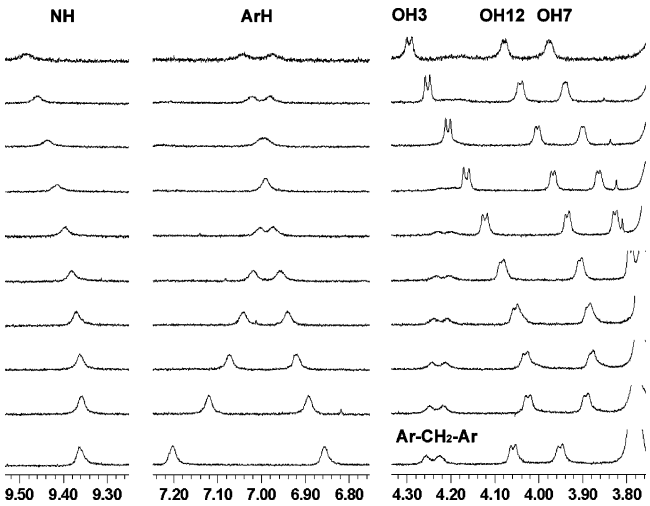

FIGURE 1. Portions of ^{1}H NMR (400 MHz) spectra of **1b** in different ratios of DMSO-d_6/CCl_4 at ambient temperature. The solvents are 100, 90, 80, 70, 60, 50, 40, 30, 20, and 10% DMSO from top to bottom. See structure of cholic acid for OH labeling.

splitting is also observed for **1b** (Figure 1, ArH), which is based on a conformationally mobile scaffold. Splitting by itself does not prove the two proposed conformers but does support a transition between two ordered conformations as the solvents go from mostly polar to mostly nonpolar. Given the binding properties mentioned previously, it is reasonable to assume that the conformer in polar solvents is micelle-like and that the one in the nonpolar solvents is reversed-micelle-like.

Cholate substitution on the calixarene clearly had a dramatic effect on the calixarene because the parent calixarene **4b** contained extremely broad peaks in the ^{1}H NMR spectrum. Since the distance between the two aromatic proton peaks correlates with the stability of the ordered, micelle-like, or reversed-micelle-like conformers based in **1a**,[8,9] we expected a smaller splitting in the less pre-organized **1b**, as part of the solvophobic interactions among the cholates needs to compensate for the loss of entropy during formation of an ordered conformation. This is indeed the case. For example, the two peaks are separated by 158 Hz for **1a** but 140 Hz for **1b** in 10% DMSO.

A change of conformation is also evident from the methylene bridge protons (Ar−CH_2−Ar), which are diagnostic of calix[4]arene conformations.[13] The "axial" protons at ∼4.2 ppm begin to appear as (part of) an AB quartet with DMSO ≈60% and become more well-formed with lower DMSO, consistent with a higher stability of the cone conformer. Conversion from a conformationally random calixarene to the cone conformer in **1b** indicates the presence of intramolecular attractions among the cholates, in agreement with the proposed reversed-micelle-like conformations. Interestingly, the appearance of the AB quartet concurs with the splitting of the aromatic peaks, implying that both changes are of the same origin. This result confirms our previous conclusion that splitting is caused by the adoption of ordered conformations (i.e., micelle-like conformation in polar solvents and the reversed-micelle-like conformation in nonpolar solvents).

The possibility of intermolecular aggregation of **1a** was ruled out previously because its ^{1}H NMR spectrum was nearly unchanged over a 0.2−15 mM concentration.[9] All the NMR experiments in the current study were performed at the lower end of the concentration range, typically about 1 mM. Aggregation should not be a problem.[15] Additional evidence against intermolecular aggregation is from the appearance of the proton signals. The broadening of peaks typically associated with intermolecular aggregation was essentially absent in all compounds studied in this paper.

Splitting of the aromatic protons occurs in **1b** at the polar end (e.g., in 100% DMSO) as well, suggesting formation of another ordered structure, most likely the micelle-like conformer. The methylene bridge protons in this case, however, do not appear as an AB quartet characteristic of the cone but are broad and nearly invisible. The original basket **1a** did not show such a difference in the polar end because calix[4]arene was already fixed as the cone by the long hexyl groups.[8,9] It seems that solvophobic interactions among the cholates are different for the normal and reversed-micelle-like conformers. This is quite likely because solvophobic interactions occur through direct contact of the cholate β faces in polar solvents for the former conformer but are probably mediated by polar solvent molecules for the latter. In other words, in the reversed-micelle-like conformer, DMSO is enriched in the interior of the molecule from the mostly nonpolar environment and serves to bridge the gap between the α faces of cholates. Direct contact of the α faces to simultaneously satisfy all hydrogen bonds in four cholates seems quite impossible, especially because the cholate backbone is bent toward the α face. In fact, mediation by polar solvents is also required in surfactant reversed micelles, which typically need to be stabilized by a small amount of water.[16] The cone conformation allows the α faces of all four cholates to be simultaneously solvated by entrapped DMSO molecules and thus should be the best for the reversed-micelle-like conformer. On the other hand, direct contact of the β faces, which is preferred by the normal-micelle-like conformer, may not be best in the cone-shaped calixarene. Given that sodium cholate frequently forms dimers in aqueous solutions,[11] it is quite possible that other conformations (such as 1,3-alternate) are equally good for solvophobic interactions; thus, no particular conformation of calixarene may be favored by the normal micelle-like conformer.

In aprotic solvents such as DMSO/CCl_4, both the NH and the OH protons are clearly visible. As shown in Figure 1, these protons generally move to high field with a decrease in DMSO percentage. Note that the doublets of the OH protons are clearly visible in all solvent mixtures (as also in Figure 4). In nonpolar solvents, aggregation would occur through hydrogen bonds and undoubtedly would complicate the OH signals. Clear OH signals thus once again provide evidence against intermolecular aggregation. Interestingly, the upfield shift seems to slow below 50−60% DMSO and even reverses for the OH protons in < 20% DMSO. The trend is more obvious when changes in the chemical shifts are plotted against DMSO percentages (Figure 2). Chemical shifts of NH and OH directly reflect the extent of

(15) One reviewer suggested dilution studies for other compounds, preferably before and after a break point in the −Δδ−DMSO% curve. These experiments represent more stringent tests for intermolecular aggregation. In our experience, aggregation is much less of a problem with a higher percentage of DMSO, as cholate derivatives are far more soluble in DMSO-rich solvents than in CCl_4-rich ones. Because the break points vary depending on whether the curve is for NH or OH (and for different OH's), we instead recorded ^{1}H NMR spectra of compounds **1a**, **1b**, **2**, **3**, **16**, **17**, and **18** in DMSO/CCl_4 (50:50) at ca. 0.1 mM or roughly 10 times diluted from the original samples. Sharp peaks similar to those at higher concentrations were found in all cases.

(16) Fendler, J. H. *Membrane Mimetic Chemistry*; Wiley: New York, 1982; Ch. 3.

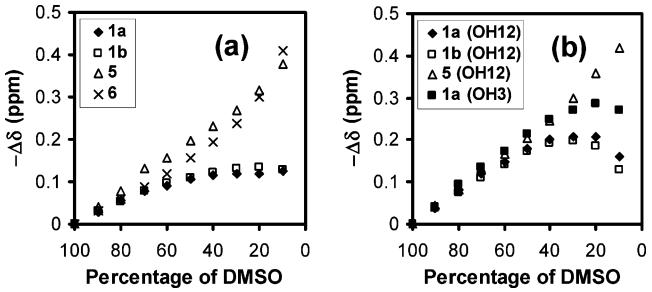

FIGURE 2. Changes in ^{1}H NMR chemical shifts of (a) NH and (b) OH as a function of solvent composition in mixtures of DMSO-d_6/CCl_4 for compounds **1a**, **1b**, **5**, and **6**. Data for OH7 sometimes cannot be obtained because of overlapping with solvent signals (as shown by Figure 1). Assignment of the OH groups is based on a 2-D COSY spectrum (Figure 1S in the Supporting Information).

hydrogen-bonding interactions involved by these protons.[17−22] In our mixed solvents, only DMSO can participate in hydrogen bonding; thus, the chemical shifts of the NH and OH groups are good indicators of the local concentration of DMSO near these groups. Figure 2a shows the relationship between $-\Delta\delta_{NH}$ and DMSO percentage for several compounds. The curves are nearly identical for monomer **5** and phenyl acetamide **6**, indicating similar solvation of amides in both compounds. Apparently, a single cholate group does not have any DMSO-enriching effect in comparison to a simple amide. Under such conditions, $-\Delta\delta_{NH}-$DMSO% simply reflects the concentration of DMSO in the bulk mixture. When multiple cholates are assembled on a calixarene, a completely different situation is observed. The $-\Delta\delta_{NH}-$DMSO% curves for **1a** and **1b** (◆ and □) initially trace those of control compounds **5** and **6** (△ and ×), suggesting that the NH groups are sensing the DMSO concentration in the bulk in high DMSO solvents just as **5** and **6**. When DMSO in the bulk drops below 50−60%, however, the curves bend downward substantially. In fact, the NH protons of **1a** and **1b** experience the same degree of hydrogen-bonding interactions (as indicated by the magnitude of $-\Delta\delta$) in 10% as in 40−50% DMSO. In other words, it seems as if 40−50% DMSO is still present near the amide protons even when the bulk solvent only contains 10% of DMSO.

The OH12 group on the cholate shows a similar downward deviation from the control curve (Figure 2b). In fact, the DMSO-enriching effect is so strong toward the low-polarity end that, as far as this hydroxyl is concerned, the local DMSO concentration actually increases when the bulk DMSO is decreased from 20 to 10%. Most interestingly, the OH3 proton, located at the periphery of the basket, shows less pronounced DMSO enrichment (■ in Figure 2b) than OH12 (◆ in Figure 2b), which is in the interior. Such a trend is more or less maintained in all of our cholate-derived compounds. This suggests that cooperativity exists between the polar groups to enrich DMSO. Among a cluster of polar groups, the ones in the center are more strongly solvated by DMSO than the ones near the edge.

Conformational changes in our amphiphilic baskets were previously hypothesized to occur as a result of preferential solvation of the hydrophilic faces of cholates by the polar solvent molecules.[8] Similar conclusions were also inferred from their guest-binding properties in response to polar solvents.[9] The $-\Delta\delta-$DMSO% curves give an estimate of the average DMSO concentration near the polar groups and provide further evidence for the formation of the reversed-micelle-like conformers. Such conformers by definition have inwardly facing polar groups and, similar to surfactant reversed micelles, should enrich polar solvents from a nonpolar environment to its interior. According to Figure 2a,b, preferential solvation (shown by deviation from control curves) seems to become important below 50−60% DMSO and is most pronounced when the solvents contain 10−20% DMSO. This effect should be even stronger below 10% DMSO. However, solubility often becomes a problem in such mixtures, precluding measurement.

For compounds **2** and **3**, splitting of the aromatic protons is hardly observable even under the most polar or nonpolar conditions. Thus, a direct connection between cholate and calixarene is needed for the splitting, and conformational insight cannot be obtained in this way. The $-\Delta\delta-$DMSO% curves for NH/OH, however, show similar DMSO enrichment as in **1a** and **1b**, suggesting the adoption of reversed-micelle-like conformations in low-polarity solvents (Figures 2S and 3S in the Supporting Information). Apparently, insertion of short spacers between cholates and calixarene does not affect the conformational changes significantly, at least for the reversed-micelle-like conformer.

The double-decker basket **8** contains two layers of cholates. With (the lower) cholates directly attached to calixarene, it displays the typical splitting of aromatic protons in both polar and nonpolar solvents (Figure 4S in the Supporting Information). The splitting, however, is consistently smaller than that in **1a** or **1b** (Figure 5S in the Supporting Information), indicating less stable micelle- or reversed-micelle-like conformations. With two layers of cholates, it is interesting to ask whether both layers participate equally in the solvent enrichment discussed previously. Fortunately, the two layers of cholates are linked by different types of amide bonds—aromatic (Ar) amides for the bottom layer and aliphatic (Alk) amides for the top, and the corresponding amide protons are well-separated in ^{1}H NMR. Interestingly, downward deviation from the control curves is still observed for the Ar amides (◆ in Figure 3a) but is completely absent for the Alk amides (□). This difference is reproducible (Figure 6S). As discussed previously, the downward deviation reflects stronger hydrogen-bonding interactions experienced by the NH/OH protons of a basket compound than those of the control and is a measure of the DMSO-enriching ability of the reversed-micelle-like conformer. The deviation has nothing to do with the nature of the amide itself because the control compounds **5** (×) and **7** (+) give similar upward curves even though they have different kinds (e.g., Ar and Alk) of amides. Therefore, the lower amides experience higher-than-usual or preferential solvation by DMSO in mostly nonpolar

(17) Pople, J. A. Schneider, W. G.; Bernstein, H. J. *High-Resolution Nuclear Magnetic Resonance*; McGraw-Hill: New York, 1959; Ch. 15.
(18) Laszlo, P. Solvent Effects and Nuclear Magnetic Resonance Spectroscopy. In *Progress in Nuclear Magnetic Resonance Spectroscopy*; Emsley, J. W., Feeney, F., Sutcliffe, L. H., Eds.; Pergamon Press: Oxford, 1967; Vol. 3, Ch. 6.
(19) Ronayne, J.; Williams, D. H. Solvent Effects in Proton Magnetic Resonance Spectroscopy. In *Annual Review of NMR Spectroscopy*; Mooney, E. F., Ed.; Academic Press: London, 1969; Vol. 2, p 83.
(20) Murthy, A. S. N.; Rao, C. N. R. Spectroscopic Studies of the Hydrogen Bond. In *Applied Spectroscopy Review*; Brame, E. G., Ed.; Dekker: New York, 1969; Vol. 2, p 69.
(21) Davis, J. C.; Deb, K. K. Analysis of Hydrogen Bonding and Related Association Equilibria by Nuclear Magnetic Resonance. In *Advances in Magnetic Resonance*; Waugh, J. S., Ed.; Academic Press: New York, 1970; Vol. 4, p 201.
(22) Konrat, R.; Tollinger, M.; Kontaxis, G.; Kräutler, B. *Monatsh. Chem.* **1999**, *130*, 961−982.

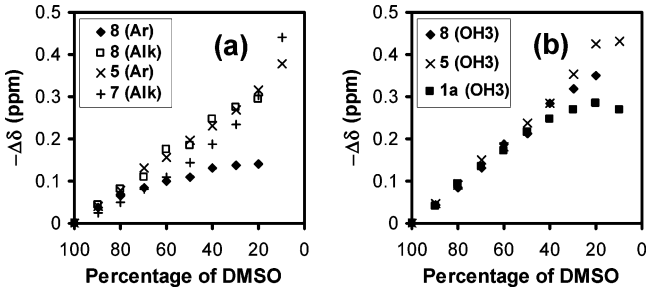

FIGURE 3. Changes in ^{1}H NMR chemical shifts of (a) NH and (b) OH as a function of solvent composition in mixtures of DMSO-d_6/CCl_4 for compounds **8**, **5**, **7**, and **1a**. Data point for 10% DMSO is missing for **8** due to insolubility.

DMSO/CCl_4 mixtures, but the top ones do not and are rather disordered.

Because of this DMSO-enriching effect, $-\Delta\delta_{NH(Ar)}$ of **8** (◆ in Figure 3a) displays a much smaller range of upfield shifts (<0.15 ppm) during solvent titration than the those of **5** or **7** (>0.4 ppm). The range is even smaller for **1a** and **1b** in Figure 2a and similarly small for **2** and **3** in Figures 2S and 3S. It should be noted that some of these $-\Delta\delta-$DMSO% curves level off but that others reverse their directions at low percentages of DMSO. Reversed curves indicate that the local concentration of DMSO increases as the overall DMSO percentage is decreased. Such a reverse is most likely caused by the onset of a conformer that is highly efficient at enriching DMSO from the environment. This is quite possible because reversing generally is absent in poorly organized baskets (also see the results in the next sections). It is clear from these $-\Delta\delta-$DMSO% curves that many basket compounds begin to experience stronger (preferential) solvation by DMSO than the control compounds early on during solvent titration. Preferential solvation occurs even in moderately polar mixtures but becomes more pronounced in mostly nonpolar mixtures such as 10% DMSO. Unfortunately, **8** is not soluble in 10% DMSO, which may be another reason that reversing is not observed for its Ar amides in Figure 3a.

Only the cholates in the top layer have hydroxyls at the C3 positions; the bottom cholates are substituted with amides at C3. A noticeable but much less significant deviation from the control (× in Figure 3b) is observed for **8** (◆) than for **1a** (■). This result suggests again that the top cholates of **8** are less organized than those of **1a**.

Conformational Changes in 1,3,5-2,4,6-Substituted Benzene-Based Molecular Baskets. In calixarene-based molecular baskets, the splitting of aromatic protons coincides with the formation of either the micelle- or reversed-micelle-like conformers. Splitting also happens in the tripodal basket **16** (Figure 4): the benzylic methylene protons at 4.2 ppm appear as an AB quartet in nonpolar solvents but as a single peak in solvents with intermediate polarity. (The peak pattern is a little complicated in some cases because of an additional small coupling to the amide proton.) As in the calixarene baskets (compare Figure 1), the reversed-micelle-like conformer seems to be better formed than the micelle-like one, as shown by a larger splitting of the benzylic protons in low DMSO mixtures than in high DMSO ones. The micelle-like conformer, as expected, can be stabilized by the addition of water, for the splitting is much more visible in D_2O/DMSO (20:80) than in pure DMSO. Overall, the magnitude of splitting is smaller in the tripodal basket than in the calixarene baskets—up to 40 Hz for **16** versus over 150 Hz for **1a**. This is the first indication that the hexasubstituted benzene is a less ideal scaffold than calix[4]-arene for these molecular baskets. The OH protons once again appear as clear doublets (except in D_2O/DMSO mixtures where they are exchanged into deuterium), suggesting the absence of intermolecular aggregation.

Splitting of benzylic protons disappears as soon as spacers are introduced between cholates and scaffold (baskets **17** and **18**). This is the same effect seen in the calixarene baskets. Hence, we turn to the $-\Delta\delta-$DMSO% curves to study the (reversed-micelle-like) conformations. To our surprise, $-\Delta\delta_{NH}$ of **16** gives a curve almost identical to that of control compound **7** (Figure 7S in the Supporting Information), seemingly suggesting no DMSO enrichment from the environment by this basket. DMSO enrichment does happen as judged by the $-\Delta\delta_{OH12}$ curves in all three tripodal baskets, as well as in the bis-armed **15** (Figure 5a), although to a smaller extent in comparison to the calixarene baskets (compare Figure 2b). This is another piece of evidence that the hexasubstituted benzene is not as good a scaffold as calix[4]arene for the molecular basket, presumably because the calix[4]arene-based baskets can better accommodate DMSO in the internal hydrophilic space with four (instead of three) cholates. Basket **16** is soluble enough in 5% DMSO. As shown in Figure 5a (+), enormous DMSO enrichment occurs under this condition, causing the internal DMSO concentration to reach nearly 50%. It seems that, for the hexasubstituted benzene-derived baskets, a large scale conformational change requires more extreme conditions due to less efficient solvophobic interactions. For example, $-\Delta\delta_{OH12}-$DMSO% curves reverse directions with 20−30% DMSO in **1b** (Figure 2b) but only below 10% in **16**.

The discrepancy between the $-\Delta\delta_{NH}$ and the $-\Delta\delta_{OH12}$ curves of **16** may come from the small size of the scaffold—the three amide groups near the hexasubstituted benzene probably are quite close in space. If DMSO molecules cannot approach the amides from the inside of the basket, the $-\Delta\delta_{NH}$ curve will only reflect DMSO concentrations in the bulk. The situation is different for OH12 groups, located farther away from the hexasubstituted benzene. With considerable flexibility between the fused steroid backbone and the base, DMSO molecules should have no difficulty entering the upper part of the basket, making OH12 groups able to sense DMSO enrichment.

The chemical shifts of the amide protons in **17** are noteworthy. Its Ar amides and Alk amides are very different in their response to DMSO percentage. Whereas the top Ar amides (△ in Figure 5b) deviate downward from that of the control **7** (+), the bottom Alk amides (▲) actually deviate upward. An upward deviation means that the $\delta_{NH(Alk)}$ of **17** is more sensitive to bulk DMSO% than that of **7**. The exact reason for this high sensitivity is unclear to us. What is clear is that the Alk amides do not experience any DMSO-enriching effect. Also, within the same molecule, the Ar amides near the cholates are less sensitive to the environmental concentration of DMSO than the Alk amides that are farther away.

For **18**, on the other hand, both the upper and the lower amide protons (■ and □ in Figure 5b) experience DMSO enrichment. Note that the rigid and flexible linkers made no difference in the calixarene baskets. But, for the hexasubstituted benzene-derived ones, it seems as if the flexible 4-aminobutyroyl linker not only allows more efficient aggregation of the cholates but also opens up space above the lower amides so that the basket can better accommodate DMSO. A possible explanation for the

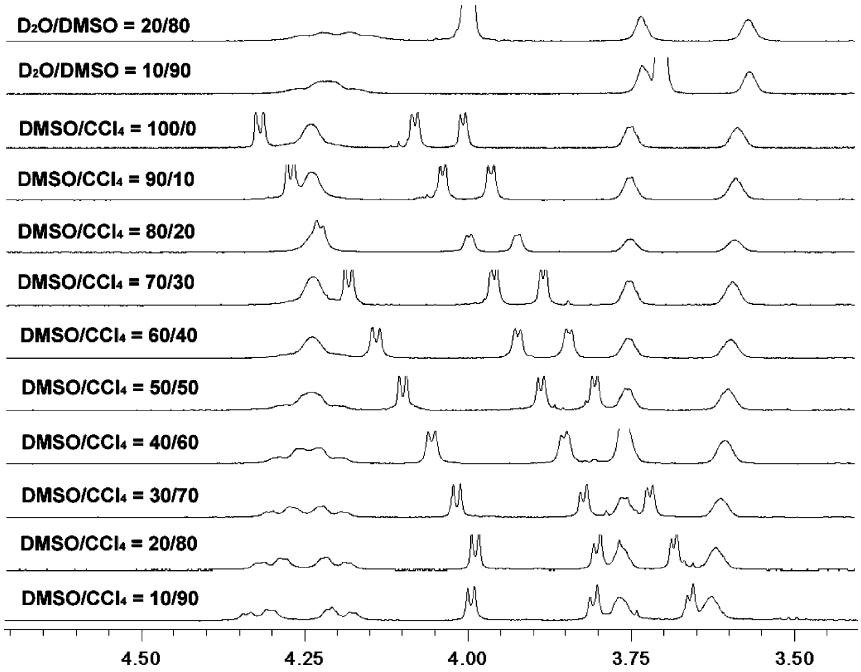

FIGURE 4. Portions of ^{1}H NMR (300 MHz) spectra of **16** in different solvents at ambient temperature. The broad singlets at 3.55−3.60 and 3.70−3.75 ppm are from protons on C12 and C3 adjacent to the hydroxyl groups.

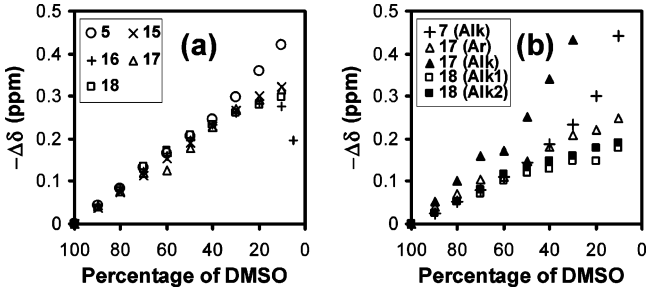

FIGURE 5. Changes in ^{1}H NMR chemical shifts of (a) OH12 for compounds **5**, **15**−**18** and (b) NH for compounds **7**, **17**, and **18** as a function of solvent composition in mixtures of DMSO-d_6/CCl_4.

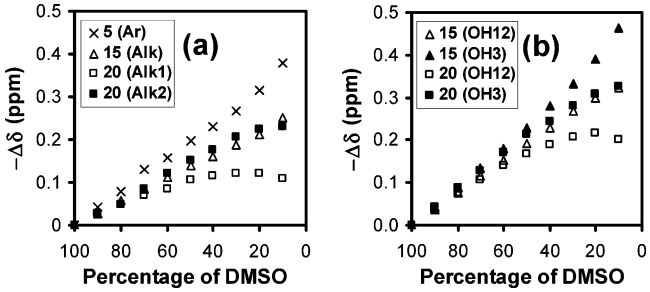

FIGURE 6. Changes in ^{1}H NMR chemical shifts of (a) NH and (b) OH for compounds **19** and **20** as a function of solvent composition in mixtures of DMSO-d_6/CCl_4.

difference between **16**/**17** and **18** lies in the position of amides relative to cholates. The solvophobic force in the baskets mostly originates from the facially amphiphilic cholates. For a compact basket (**16**) or one with rigid spacers (**17**), the solvophobic force among the cholates will compress the structure and cause the amide protons at the bottom to move closer. For a basket with a flexible spacer (**18**), however, interactions among the cholates may be insulated from the lower amides and do not change their arrangements significantly. It is even possible that the crowdedness near the lower amides in **16**/**17** may not come from the size of the scaffold but actually from the solvophobic force of the cholates.

Double-decker basket **19** represents the worst combination—hexasubstituted benzene as a poor scaffold (in comparison to calix[4]arene) and the cholate dimer as poor wall material (in comparison to monomeric cholate). Not surprisingly, negligible extent of DMSO enrichment is seen in either $-\Delta\delta_{NH}$ or $-\Delta\delta_{OH}$ curves (Figure 8S in the Supporting Information). However, when six cholates are arranged within one layer as in dendritic basket **20** instead of in two layers in **19**, a different result is obtained. The top and bottom amide protons in **20** initially overlap and respond to the DMSO percentage similarly as the amide in the control **15** but very soon split to give two curves, whereas the bottom amides (three protons by integration, ■ in Figure 6a) follow the same track of amides in **15** (△), and the top amides (six protons, □) give a larger downward deviation. Since **20** is essentially made of three units of **15**, amides in the latter and the top amides of the former should behave similarly if only the cholates attached to the same phenyl ring can interact. The fact that **20** can enrich DMSO much more efficiently than part of its structure clearly indicates that DMSO enrichment by cholates is a cooperative phenomenon and that all six cholates work together to enrich DMSO instead of as three pairs. Also, it appears that, as long as a sufficient number of cholates is present to form an enclosed space, the reversed-micelle-like conformer can be reasonably stable. Cooperativity is also obvious from the $-\Delta\delta_{OH}$ curves (Figure 6b). On the basis of both OH12 protons located in the center of the baskets and OH3 near the periphery, basket **20** (□ and ■) is better able to enrich DMSO than control **15** (△ and ▲). For the same basket, the OH12 protons are less sensitive to changes in solvent composition than OH3. As mentioned previously, this is the same trend observed for all the baskets synthesized in this paper and is additional evidence for the cooperativity in DMSO enrichment.

Finally, this contrast between **20** and **15** also suggests that the changes in the NH/OH chemical shifts are not caused by

simple intramolecular hydrogen bonding with other NH/OH protons—otherwise, **20** and **15** would behave the same. Another piece of evidence against this intramolecular hydrogen-bonding mechanism is the nearly identical $-\Delta\delta_{NH}$—DMSO% curves of **19** and **5** (Figure 8S, part a). It is difficult to imagine that intramolecular hydrogen bonds can have the exact same effect on the $\delta_{NH/OH}$ of **19**, a highly complex molecule, as DMSO in the bulk has on that of **5**, a monomeric cholate incapable of intramolecular hydrogen bonds (at least for the NH proton).

Conclusion

Multiple cholates attached to a covalent scaffold can readily aggregate intramolecularly to form unimolecular micelles and reversed micelles. The micelle-like conformer prefers direct contact of the hydrophobic β faces of cholates and seems to be best formed in tight structures. The reversed-micelle-like conformer is mediated by polar solvent molecules entrapped in the interior of the molecule and can tolerate significant modification of structures. Among the two scaffolds investigated, calix[4]arene gives baskets that can better enrich polar solvents than 1,3,5-2,4,6-hexasubstituted benzene from a mostly nonpolar solvent mixture. The difference may simply be caused by the number of arms (four vs three) in the two scaffolds. When branched spacers are introduced into the latter scaffold to increase the number of interacting cholates (e.g., basket **20**), an enclosed space for DMSO accommodation can be easily formed, and the reversed-micelle-like conformer is quite stable.

The calix[4]arene-derived baskets can also tolerate spacers better than the 1,3,5-2,4,6-hexasubstituted benzene derivatives. Both rigid 4-aminobenzoyl and flexible 4-aminobutyroyl spacers afford stable reversed-micelle-like conformers in calix[4]arene-based baskets. Baskets constructed from the hexasubstituted benzene, on the other hand, prefer flexible spacers, which seem to promote more efficient intramolecular aggregation of the cholates. The α,β-cholate dimer (**13**) does not seem to be a good wall material for the basket. Although the bottom cholates directly attached to the scaffold can be organized by entrapped polar solvents, the top cholates are quite disordered. This is probably an entropic effect—as the cholates move farther away from the scaffold, it is more difficult for solvophobic interactions to constrain their movements.

Experimental Procedures

General Methods. See the Supporting Information.

Compounds 4a, 4b, and 1a. See the Supporting Information.

Compound 1b. Cholic acid (349.3 mg, 0.855 mmol), **4b** (105.0 mg, 0.194 mmol), and benzotriazol-1-yloxytris(dimethylamino)-phosphonium hexafluorophosphate (BOP, 412.4 mg, 0.931 mmol) were dissolved in anhydrous DMF (15 mL) in N_2. Diisopropylethylamine (DIPEA, 238.0 mg, 1.707 mmol) was added via a syringe. The reaction mixture was stirred at 50 °C for 18 h. The solution was poured into brine (50 mL). The precipitate was filtered, washed with water (2 × 10 mL) and CH_3CN (5 mL), and purified by preparative TLC (SiO_2, $CHCl_3/CH_3OH$ = 8:1) to give a white powder (301.9 mg, 0.144 mmol, 74% yield). ^{1}H NMR (DMSO-d_6/CCl_4 = 1:1, 400 MHz, δ): 9.36 (s, 4H), 7.20 (s, 4H), 6.86 (s, 4H), 4.24 (d, 4H, J = 11.6 Hz), 4.06 (d, 4H, J = 4.4 Hz), 3.95 (d, 4H, J = 4.0 Hz), 3.78 (m, 16H), 3.62 (s, 4H), 3.18 (s, 4H), 3.10 (d, 4H, J = 12.4 Hz), 2.19−0.75 (m, 124H), 0.61 (s, 12H). ^{13}C NMR (75 MHz, CD_3OD, δ): 171.6, 153.9, 134.2, 134.1, 119.9, 71.5, 70.9, 66.8, 46.7, 46.2, 42.0, 41.8, 35.8, 35.4, 34.9, 33.9, 32.0, 30.9, 29.1, 27.8, 26.7, 23.3, 23.1, 17.6, 12.9. MALDI-TOFMS (m/z): $[M + Na]^+$ calcd for $C_{128}H_{187}N_4O_{20}Na$: 2125.9; found: 2128.6.

Compound 2. Acid **21** (450 mg, 0.854 mmol, see the Supporting Information for its synthesis), **4a** (159 mg, 0.194 mmol), and BOP (378 mg, 0.854 mmol) were dissolved in anhydrous DMF (10 mL). DIPEA (220 mg, 1.708 mmol) was added via a syringe. The reaction mixture was stirred at 50 °C for 20 h and was precipitated in acetone (100 mL). The precipitate was filtered, washed with acetone (2 × 10 mL), and purified by preparative TLC (SiO_2, $CHCl_3/CH_3OH$ = 4:1) to give a white powder (250.4 mg, 45% yield). ^{1}H NMR (DMSO-d_6/CCl_4 = 1:1, 300 MHz, δ): 10.04 (s, 4H), 9.77 (s, 4H), 7.79 (d, 8H, J = 9.0 Hz), 7.59 (d, 8H, J = 8.4 Hz), 4.32 (s, 8H), 4.11 (s, 4H), 4.00 (d, 4H, J = 2.1 Hz), 3.80 (m, 8H), 3.60 (m, 4H), 3.15 (m, 8H), 2.30−0.79 (m, 168H), 0.57 (s, 12H). ^{13}C NMR (75 MHz, DMSO-d_6/CCl_4 = 1:1, δ): 174.1, 166.6, 153.6, 141.9, 135.2, 132.2, 129.7, 128.4, 121.8, 119. 7, 77.8, 75.7, 73.2, 71.7, 68.3, 47.0, 46.5, 35.4, 34.9, 34.7, 34.2, 32.3, 32.0, 31.27, 31.25, 30.4, 30.1, 28.3, 27.74, 26.5, 26.2, 23.3, 23.0, 22.5, 17.3, 14.1, 12.5. MALDI-TOFMS (m/z): $[M + Na]^+$ calcd for $C_{176}H_{247}N_8O_{24}Na$: 2881.9; found: 2881.8.

Compound 3. Acid **22** (264.6 mg, 0.536 mmol, see the Supporting Information for its synthesis), **4a** (100.1 mg, 0.122 mmol), and BOP (237.4 mg, 0.536 mmol) were dissolved in anhydrous DMF (10 mL) in N_2. DIPEA (138 mg, 1.072 mmol) was added via a syringe. The reaction mixture was stirred at 50 °C for 20 h and was precipitated in acetone (50 mL). The precipitate was filtered, washed with acetone (2 × 10 mL), and purified by preparative TLC (SiO_2, $CHCl_3/CH_3OH$ = 4:1) to give a white powder (120.2 mg, 36% yield). ^{1}H NMR (DMSO-d_6/CCl_4 = 1:1, 300 MHz, δ): 9.45 (s, 4H), 7.76 (s, 4H), 6.89 (d, 8H, J = 4.0 Hz), 4.32 (m, 8H), 4.09 (s, 4H), 4.00 (s, 4H), 3.75 (s, 8H), 3.57 (s, 4H), 3.14 (m, 8H), 2.99 (m, 12H), 2.24−0.77 (m, 168H), 0.54 (s, 12H). ^{13}C NMR (75 MHz, DMSO-d_6/CCl_4 = 1:1, δ): 173.2, 170.8, 152.4, 134.7, 133.8, 120.2, 75.6, 71.7, 71.1, 66.9, 46.8, 46.4, 42.2, 42.0, 38.8, 36.0, 35.9, 35.6, 35.1, 34.3, 33.4, 32.4, 32.4, 31.1, 30.4, 29.2, 28.0, 26.9, 26.2, 26.0, 23.5, 23.3, 23.1, 17.8, 14.6, 13.0. MALDI-TOFMS (m/z): $[M + H]^+$ calcd for $C_{164}H_{255}N_8O_{24}$: 2723.8; found: 2725.9.

Compound 5 and 10−12. See the Supporting Information.

Compound 13. Cholic acid (510 mg, 1.25 mmol), amine **12** (530 mg, 1.25 mmol), and BOP (663 mg, 1.5 mmol) were dissolved in anhydrous DMF (8 mL). DIPEA (0.70 mL, 4.5 mmol) was added with a syringe. The reaction mixture was stirred at room temperature for 9 h. The mixture was concentrated to about 4 mL in vacuo. The residue was triturated with ice water, filtered, washed with water twice, and dried by air suction. The crude product was purified by column chromatography over silica gel using CH_2Cl_2/MeOH (20:1) as the eluents to obtain 755 mg of light yellow solid (75% yield). ^{1}H NMR (400 MHz, $CDCl_3/CD_3OD$ = 1:1, δ): 4.05−3.98 (m, 3H), 3.83 (br, 2H), 3.62 (s, CO_2CH_3, 3H), 3.42−3.85 (br, 1H), 2.58−0.85 (series of m, 60H), 0.65 (br, 6H). ^{13}C NMR (100 MHz, $CD_3OD/CDCl_3$ = 1:1, δ): 175.3, 174.5, 72.7, 72.6, 71.2, 67.9, 67.8, 51.1, 46.6, 46.0, 45.4, 41.33, 41.26, 39.1, 38.9, 36.8, 35.2, 35.1, 35.0, 34.9, 34.5, 34.3, 33.9, 33.0, 32.9, 31.8, 30.73, 30.67, 29.5, 28.1, 27.8, 27.3, 27.2, 26.1, 25.6, 24.0, 22.9, 22.5, 22.0, 16.6, 12.0. MALDI-TOFMS (m/z): $[M + Na]^+$ calcd for $C_{49}H_{81}NNaO_8$, 835.17; found, 834.09.

Compound 8. Compound **13** was hydrolyzed by aqueous LiOH (1 M) in MeOH. The acid obtained (2.10 g, 2.63 mmol) and *N*-hydroxysuccinimide (0.364 g, 3.16 mmol) were dissolved in anhydrous THF (100 mL), and 1,3-dicyclohexylcarbodiimide (DCC, 0.652 g, 3.16 mmol) in anhydrous THF (5 mL) was added. After 24 h under N_2, the white precipitate formed was removed by filtration. The filtrate was concentrated to about 10 mL and precipitated into CH_3CN. A portion of the *N*-hydroxylsuccimide ester derivative (158 mg, 0.176 mmol) and **4a** (29.0 mg, 0.035 mmol) were dissolved in anhydrous DMF (2 mL). After 32 h at 120 °C under N_2, the mixture was precipitated into CH_3CN (50 mL). The solid was collected by suction filtration and purified by

column chromatography over silica gel using $CHCl_3$/MeOH/Et_3N (20:1:0.1) as the eluent to a light yellow solid (58 mg, 40% yield). ^1H NMR (300 MHz, DMSO-d_6, δ): 9.38 (br, 4H), 7.44 (br, 4H), 6.90 (br, 4H), 4.32 (m, 8H), 4.05−3.96 (m, 16H), 3.79−3.65(br, 12H), 3.56 (br, 8H), 2.42−0.76 (series of m, 240H), 0.56 (br, 24H). ^{13}C NMR (75 MHz, $CDCl_3/CD_3OD$ = 1:1, δ): 174.4, 172.9, 152.7, 134.4, 131.9, 120.8, 75.0, 72.5, 71.1, 67.6, 46.4, 46.0, 45.9, 45.3, 41.2, 39.1, 38.7, 36.7, 35.1, 34.9, 34.7, 34.3, 34.2, 33.9, 32.7, 31.7, 30.5, 29.8, 29.5, 28.0, 27.8, 27.2, 26.0, 25.6, 23.9, 22.8, 22.4, 22.3, 21.9, 16.6, 16.5, 13.4, 11.8. MALDI-TOFMS (*m*/*z*): $[M + H]^+$ calcd for $C_{244}H_{385}N_8O_{32}$, 3942.69; found, 3942.97. $[M + Na]^+$ calcd for $C_{244}H_{384}N_8NaO_{32}$, 3963.69; found, 3961.67.

Compound 15. Compound **24** (277 mg, 1.0 mmol, see the Supporting Information for its synthesis), *N*-hydroxysuccinimide ester of cholic acid (1.20 g, 2.4 mmol, see the Supporting Information for its synthesis), and DIPEA (0.55 mL, 3.0 mmol) were dissolved in anhydrous DMF (10 mL). After 12 h at 60 °C under N_2, the mixture was concentrated in vacuo and poured into CH_3CN (25 mL). The solid was collected by suction filtration and purified by column chromatography over silica gel using $CHCl_3$/MeOH/H_2O (5:1:0.1) as the eluents to give a white solid (0.52 g, 50% yield). ^1H NMR (300 MHz, DMSO-d_6, δ): 8.38 (t, 2H), 7.68 (s, 2H), 7.34 (s, 1H), 4.30 (d, 2H), 4.25 (s, 4H), 4.09 (d, 2H), 4.00 (d, 2H), 3.81 (s, 3H), 3.75 (s, 2H), 3.58(s, 2H), 3.22−3.09 (m, 2H), 2.30−1.85 (m, 12H), 1.84−1.51 (m, 14H), 1.49−0.70 (m, 34H), 0.53 (s, 6H). ^{13}C NMR (75 MHz, CD_3OD, δ): 175.54, 167.01, 140.09, 131.45, 130.69, 127.15, 72.82, 71.70, 67.85, 54.67, 51.57, 46.91, 46.32, 42.45, 42.02, 41.81, 39.94, 39.29, 35.67, 35.34, 35.34, 34.74, 32.97, 32.21, 30.03, 28.43, 27.55, 26.70, 25.13, 23.10, 22.06, 18.18, 16.61, 11.89. MALDI-TOFMS (*m*/*z*): $[M + Na]^+$ calcd for $C_{58}H_{90}N_2NaO_{10}$, 998.33; found, 997.82; $[M + K]^+$ calcd for $C_{58}H_{90}N_2KO_{10}$, 1014.44; found, 1014.06.

Compound 16. Cholic acid triformate (396 mg, 0.804 mmol) was dissolved in dry CH_2Cl_2 (20 mL). Oxalyl chloride (0.20 mL, 6.88 mmol) was added via a syringe, followed by two drops of dry DMF. The mixture was stirred at room temperature under N_2 flush for 1.5 h. Solvents were removed in vacuo. Dry CH_2Cl_2 (2 × 5 mL) was added and evaporated again in vacuo. The residue was dissolved in dry CH_2Cl_2 (30 mL) and was added to a stirred suspension of amine **14** (61.4 mg, 0.246 mmol) and Et_3N (0.2 mL, 1.4 mmol) in anhydrous THF (5 mL). After 1 h at room temperature, solvents were evaporated in vacuo. The residue was combined with K_2CO_3 (1.150 g, 8.3 mmol) and MeOH (30 mL). The mixture was heated to reflux for 17 h. The solvent was evaporated, and the residue was purified by column chromatography over silica gel using $CHCl_3$/MeOH (5:1) to give a white glass (238 mg, 68%). ^1H NMR (300 MHz, CD_3OD/CCl_4 = 8:2, δ): 4.40 (s, 6H), 3.92 (br, 3H), 3.79 (br, 3H), 3.40−3.30 (m, 3H), 2.73 (q, 6 H, J = 7.4 Hz), 2.28−0.88 (m, 99H), 0.70 (s, 9H). ^{13}C NMR (75 MHz, CD_3OD/CCl_4 = 8:2, δ): 174.8, 144.0, 131.8, 72.9, 71.6, 67.9, 55.0, 46.7, 46.4, 41.9, 41.8, 39.8, 39.2, 38.0, 35.7, 35.6, 34.9, 34.8, 33.4, 32.5, 32.0, 30.0, 28.4, 27.7, 26.6, 23.3, 22.9, 22.6, 17.0, 16.0, 12.4. MALDI-TOFMS (*m*/*z*): $[M + Na]^+$ calcd for $C_{87}H_{141}N_3NaO_{12}$, 1444.05; found, 1438.90; $[M + K]^+$ calcd for $C_{87}H_{141}KN_3O_{12}$, 1460.16; found, 1456.04.

Compound 17. Acid **21** (204.9 mg, 0.388 mmol), amine **14** (32.2 mg, 0.129 mmol), tetramethyluronium hexafluorophosphate (HBTU, 176.6 mg, 0.466 mmol), and DIPEA (398.6 mg, 3.08 mmol) were dissolved in dry DMF (4 mL). The mixture was heated at 90 °C under N_2 for 24 h. The mixture was precipitated into CH_3CN (50 mL). The solid was collected by suction filtration and was purified by column chromatography over silica gel using $CHCl_3$/MeOH/H_2O (5:1:0.1) to give an off powder (150.3 mg, 65%). ^1H NMR (400 MHz, d_6-DMSO, δ): 10.05 (s, 3H), 8.16 (s, 3H), 7.80 (d, 6H, J = 8.6 Hz), 7.59 (d, 6H, J = 8.6 Hz), 4.52 (br, 6H), 4.32 (d, 3H, J = 4.2 Hz), 4.12 (d, 3H, J = 3.1 Hz), 4.02 (d, 3H, J = 3.1 Hz), 3.77 (br, 3H), 3.59 (br, 3H), 3.16 (br, 3H), 2.88−2.71 (br, 6H), 2.41−0.74 (m, 99H), 0.56 (s, 9H). ^{13}C NMR (100 MHz, d_6-DMSO, δ): 172.8, 166.2, 144.4, 142.6, 132.7, 129.1, 129.0, 118.6, 71.7, 71.1, 66.9, 46.8, 46.4, 42.2, 42.1, 36.0, 35.9, 35.6, 35.1, 34.2, 32.1, 31.1, 29.3, 28.0, 26.9, 23.5, 23.3, 17.9, 17.0, 13.1. MALDI-TOFMS (*m*/*z*): $[M + Na]^+$ calcd for $C_{108}H_{156}N_6NaO_{15}$, 1801.42; found, 1794.39; $[M + K]^+$ calcd for $C_{108}H_{156}KN_6O_{15}$, 1801.42; found, 1817.52.

Compound 18. Acid **22** (614.1 mg, 1.244 mmol), amine **14** (70.5 mg, 0.283 mmol), and BOP (601.7 mg, 1.358 mmol) were dissolved in anhydrous DMF (15 mL). DIPEA (323 mg, 2.321 mmol) was added via a syringe. The reaction mixture was stirred at 50 °C for 20 h. The compound was precipitated in brine (50 mL), filtered, and washed with water (2 × 10 mL). The residue was purified by preparative TLC (SiO_2, CH_3Cl/CH_3OH = 4:1) to give a white powder (312.3 mg, 0.187 mmol, 66% yield). ^1H NMR (DMSO-d_6, 400 MHz, δ):? 7.72 (m, 3H), 4.29 (d, 3H, J = 4.0 Hz), 4.24 (s, 6H), 4.07 (d, 3H, J = 2.4 Hz), 4.06 (s, 3H), 3.98 (d, 3H, J = 2.8 Hz), 3.74 (s, 3H), 3.57 (s, 3H), 2.94 (q, 6H, J = 6.0 Hz), 2.63 (m, 6H), 2.08−0.78 (m, 102H), 0.56 (s, 9H). ^{13}C NMR (75 MHz, DMSO-d_6, δ): 175.55, 173.61, 143.88, 131.64, 72.66, 71.51, 67.66, 48.49, 46.66, 46.12, 41.83, 41.65, 39.66, 39.10, 38.45, 37.52, 35.57, 35.14, 34.55, 32.83, 32.03, 29.83, 28.25, 27.41, 26.51, 25.64, 22.91, 22.61, 21.86, 16.41, 15.29, 11.70. MALDI-TOFMS: calcd. for $C_{99}H_{161}N_6O_{15}Na$ $[M + Na]^+$: 1698.4; found: 1693.0.

Compound 19. A portion of the *N*,*N*-hydroxysuccinimide ester derivative of **13** (573 mg, 0.64 mmol, prepared as in the synthesis of **8**) and amine **14** (50.0 mg, 0.2 mmol) were dissolved in anhydrous DMF (5 mL); the reaction mixture was stirred at 60 °C under N_2. After 26 h, the mixture was precipitated in CH_3CN (50 mL). The solid was collected by suction filtration and purified by column chromatography over silica gel using $CHCl_3$/MeOH/Et_3N (20:1:0.1) as the eluents (467 mg, 65% yield). ^1H NMR (300 MHz, DMSO-d_6, δ): 7.71 (br, 3H), 7.50 (br, 3H), 4.18−4.09 (m, 9H), 4.05−3.98 (m, 12H), 3.83−3.65 (br, 9H), 3.59 (br, 6H), 3.08 (br, 3H), 2.62 (br, 3H), 2.22−1.34 (series of m, 180H), 0.58 (br, 18H). ^{13}C NMR (75 MHz, $CD_3OD/CDCl_3$ = 1;1, δ): 174.40, 174.41, 143.44, 131.13, 72.46, 71.04, 67.53, 60.05, 51.57, 46.36, 45.80, 45.18, 41.13, 38.99, 38.63, 32.66, 32.54, 32.17, 31.67, 31.62, 30.33, 29.38, 27.93, 27.68, 27.09, 25.90, 25.41, 23.82, 22.64, 22.16, 21.76, 19.89, 16.34, 15.35, 13.18, 11.71. MALDI-TOFMS (*m*/*z*): $[M + Na]^+$ calcd for $C_{159}H_{258}N_6NaO_{21}$, 2612.78; found, 2612.03.

Compound 20. Ester **15** was hydrolyzed by aqueous LiOH (1 M) in MeOH. A portion of the solid (234 mg, 0.24 mmol) was combined with amine **14** (20 mg, 0.08 mmol), BOP (143 mg, 0.314 mmol), and DIPEA (0.07 mL, 0.40 mmol) in DMF (5 mL). After 24 h at 60 °C under N_2, the solvent was removed in vacuo, and the residue was slowly added to CH_3CN (15 mL). The solid was purified by column chromatography over silica gel using $CHCl_3$/MeOH/Et_3N (5:1:0.1) as the eluent to give a white solid (125 mg, 50% yield). ^1H NMR (300 MHz, DMSO-d_6, δ): 8.29 (t, 9H), 7.60 (s, 6H), 7.18 (s, 3H), 4.52 (s, 6H), 4.32 (d, 6H), 4.20 (s, 12H), 4.09 (d, 6H), 4.00 (d, 6H), 3.75 (s, 6H), 3.58(s, 6H), 3.22−3.09 (m, 6H), 2.30−1.85 (m, 36H), 1.84−1.51 (m, 42H), 1.49−0.70 (m, 102H), 0.54 (s, 18H). ^{13}C NMR (75 MHz, CD3OD, δ): 175.5, 168.6, 144.7, 139.7, 134.7, 131.4, 130.3, 125.6, 124.2, 73.0, 71.7, 69.2, 46.9, 46.6, 46.5, 43.0, 41.8, 39.7, 39.3, 35.7, 34.9, 33.1, 32.0, 30.1, 28.4, 27.7, 26.6, 23.3, 22.5, 17.1, 16.2, 12.4, 8.8. MALDI-TOFMS (*m*/*z*): $[M + Na]^+$ calcd for $C_{186}H_{285}N_9NaO_{27}$, 3102.29; found, 3102.35.

Acknowledgment. Acknowledgment is made to the donors of Petroleum Research Fund, administered by the American Chemical Society, and to Iowa State University for support of this research.

Supporting Information Available: General method of the experiments, synthetic procedures, and figures. This material is available free of charge via the Internet at http://pubs.acs.org.

JO0607663